Electronic Supplementary Material (ESI) for Nanoscale.

Electronic supplementary information (ESI)

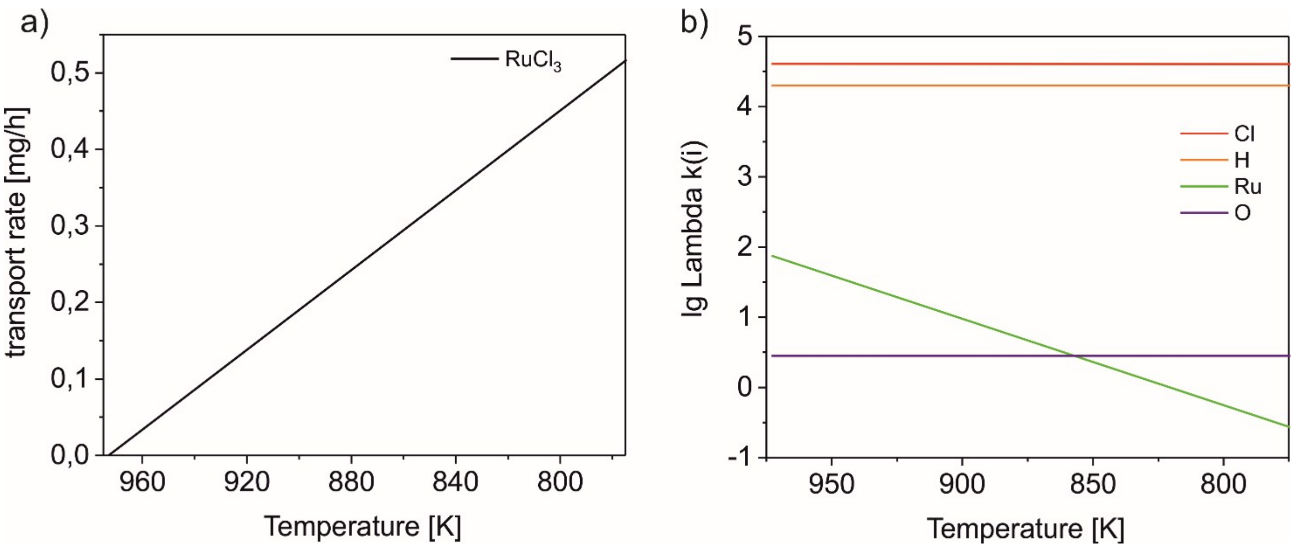

Figure 1: Thermodynamic modelling of the chemical vapor transport with TRAGMIN, a) transport rate of the deposited α-$RuCl_3$ nanosheets b) solubility of components in the gas phase

We obtain that there are mainly four transport relevant species with partial pressures higher than -5 atm (with respect to the logarithmic application of values), indicating the transport relevant edge. These are Cl_2, Cl (from homogenous equilibrium: $Cl_2(g) \rightleftarrows 2\,Cl(g)$, $RuCl_4$ and $RuCl_3$. Despite the fact in real environments are always small impurities of oxygen and/or water, no consequences to the contamination of the deposited crystals (e. g. formation of oxychlorides) could be observed by calculation. Hydrogen does not participate in the transport and is only needed for possible reduction of RuO_2 and $RuCl_3$. The transport rate indicating a relatively low magnitude with around 0,5 mg/h, supporting the formation of nanocrystals too. Highlighting the transport efficiencies we find that Cl_2 act as the transport agent (negative slope) and $RuCl_3$, as well as $RuCl_4$, as the transport efficient gas species, indicating that there is a small amount of an autotransport process that increases with rising temperature.

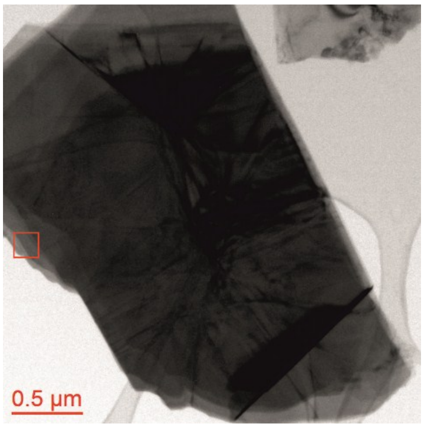

Figure 2: BFTEM image of analyzed α-$RuCl_3$ nanosheet, the red inset indicating the investigated area

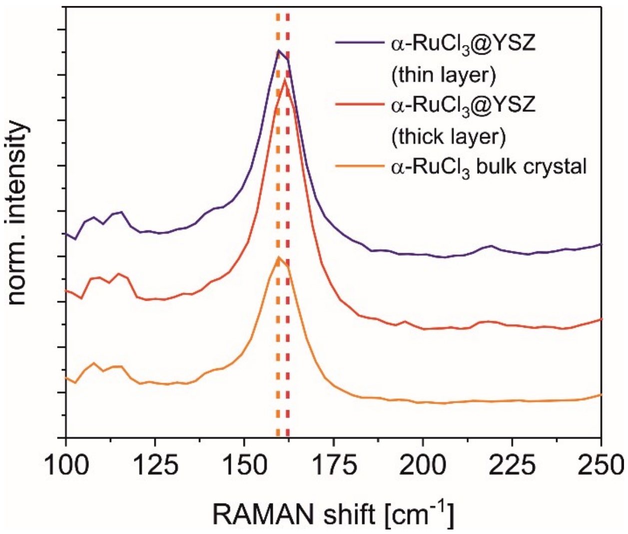

Figure 3: micro-RAMAN measurement of bulk α-$RuCl_3$ crystals (orange), α-$RuCl_3$ sheets deposited on YSZ substrates (red and blue) and indicated slight RAMAN shift

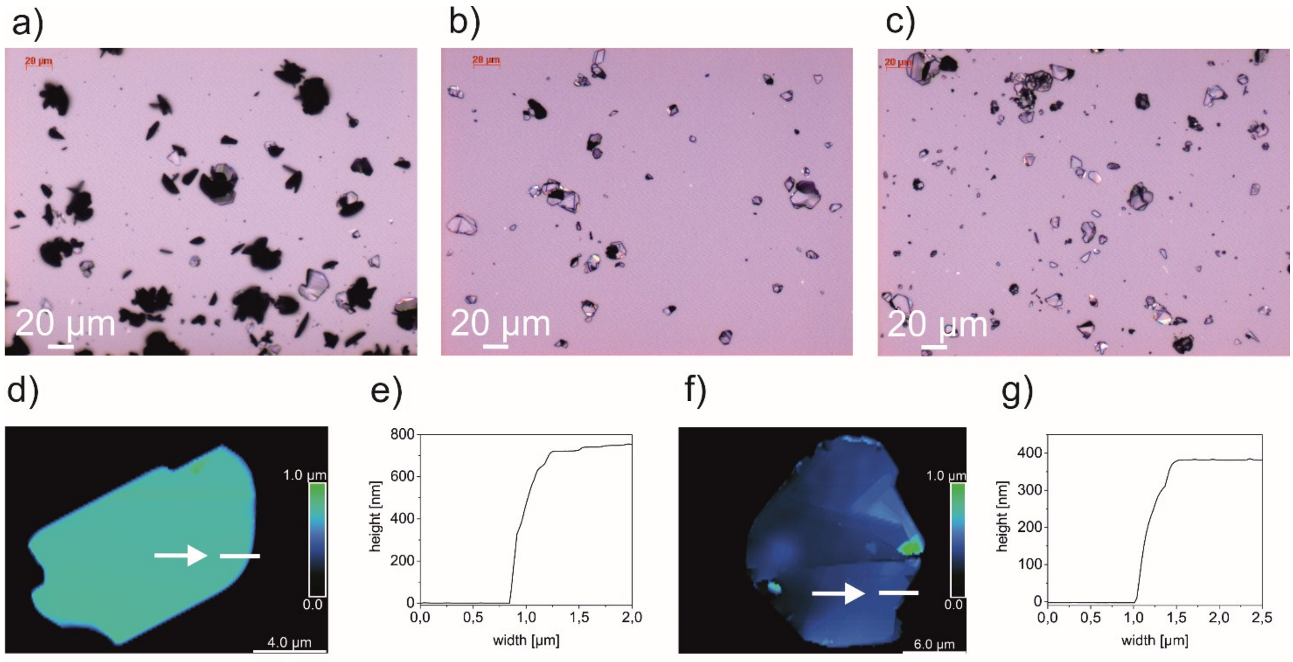

Figure 4: a) YSZ substrate with deposited α-$RuCl_3$ nanocrystals before ultrasonication; b) after 30 seconds of ultrasonication with distilled water, c) after 3 minutes of ultrasonication with distilled water, d) investigated α-$RuCl_3$ nanocrystal by means of AFM (the white line is indicating the AFM measurement), e) AFM height profile of d), f) investigated α-$RuCl_3$ nanocrystal by means of AFM (the white line is indicating the AFM measurement) and g) AFM height profile of f)

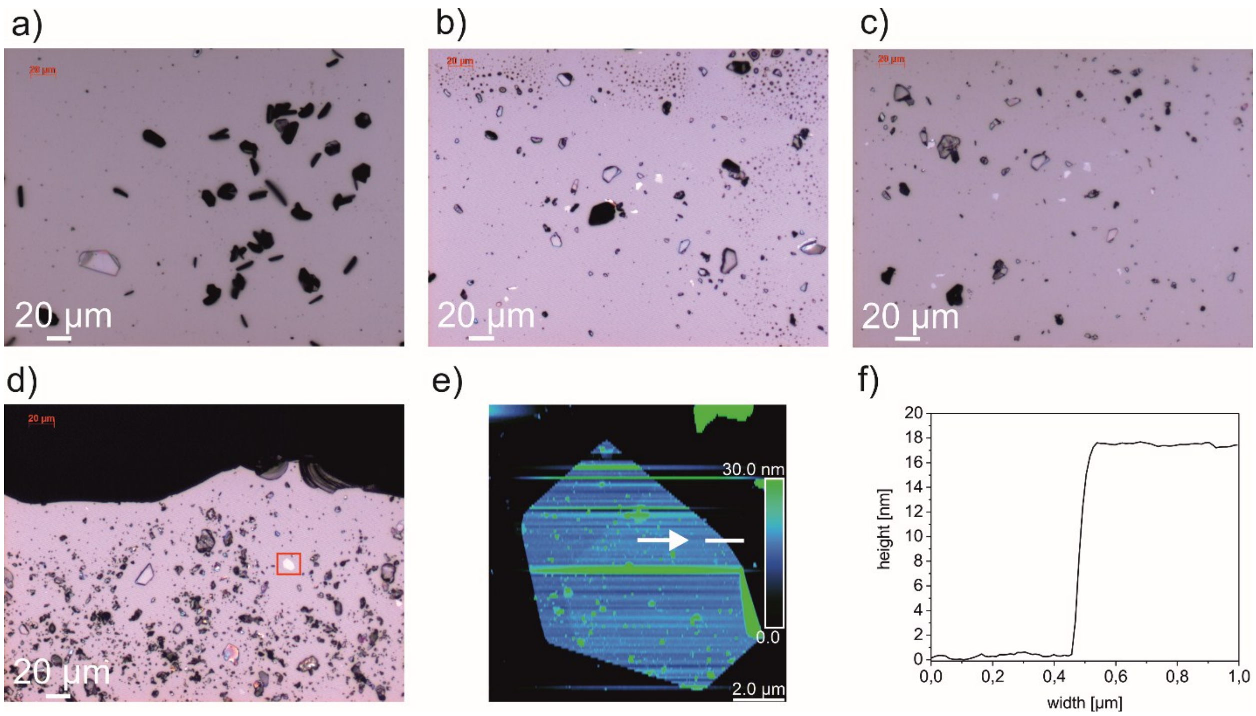

Figure 5: a) YSZ substrate with deposited α-$RuCl_3$ nanocrystals before ultrasonication; b) after 30 seconds of ultrasonication with n-hexane, c) after 3 minutes of ultrasonication with n-hexane, d) investigated α-$RuCl_3$ nanocrystal by means of AFM (the red area is indicating to location of the measurement), e) investigated α-$RuCl_3$ nanocrystal by means of AFM (the white line is indicating the AFM measurement) and f) AFM height profile of e)

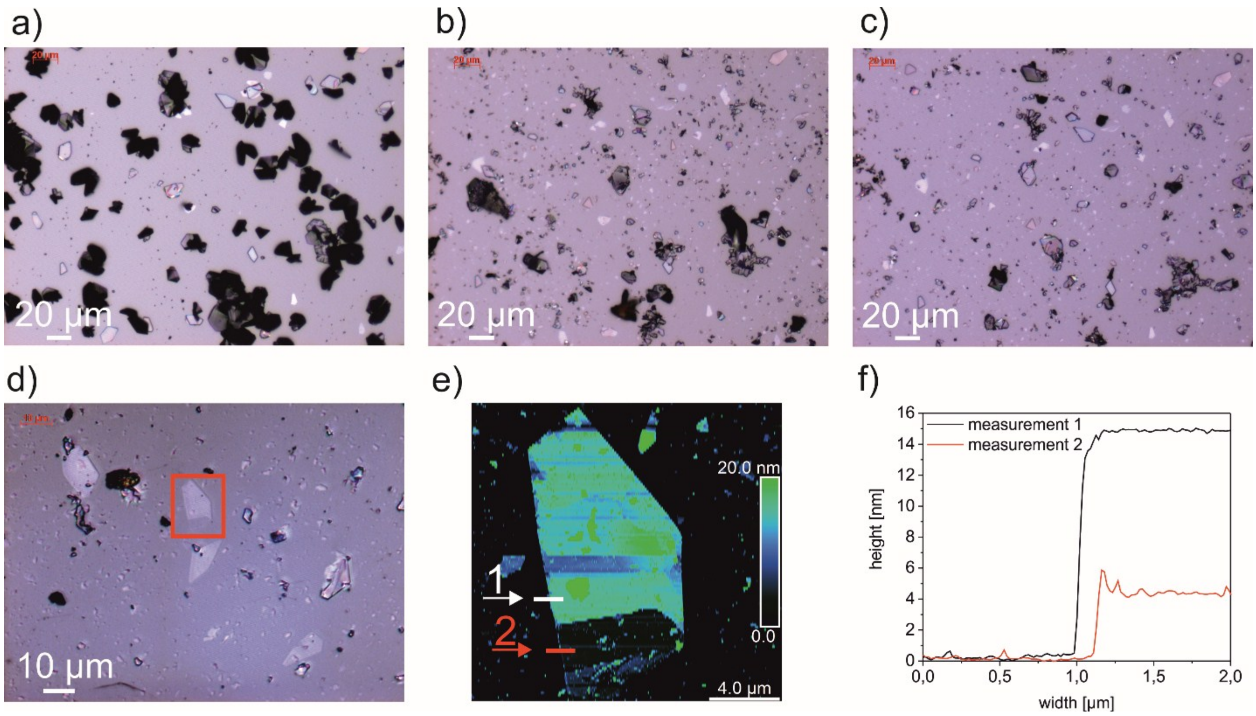

Figure 6: a) YSZ substrate with deposited α-$RuCl_3$ nanocrystals before ultrasonication; b) after 30 seconds of ultrasonication with benzene, c) after 3 minutes of ultrasonication with benzene, d) investigated α-$RuCl_3$ nanocrystal by means of AFM (the red area is indicating to location of the measurement), e) investigated α-$RuCl_3$ nanocrystal by means of AFM (the white and red lines are indicating the AFM measurements) and f) AFM height profiles of e)

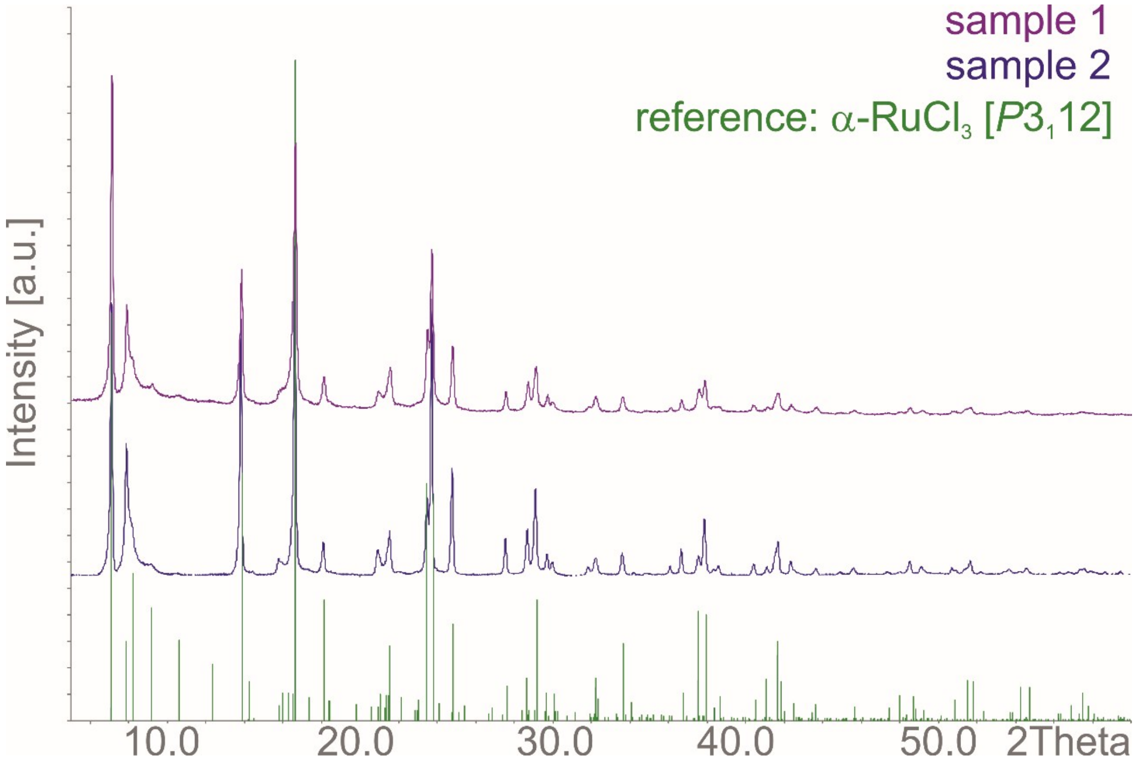

Figure 7: XRD measurements of deposited α-$RuCl_3$ crystals (blue and purple) and comparison with literature data for α-$RuCl_3$ with trigonal space group $P3_112$ (dark green)

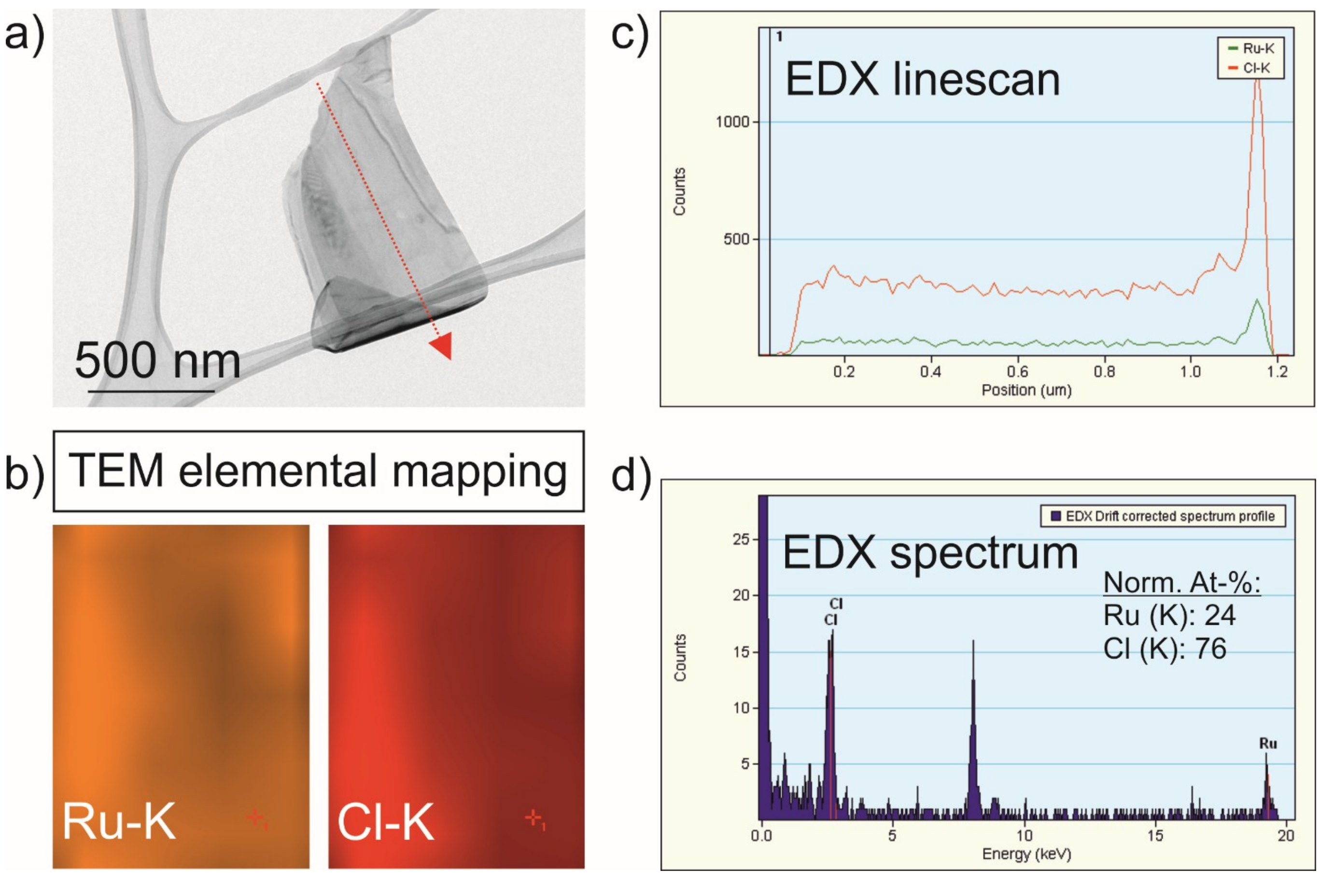

Figure 8: TEM investigation of α-$RuCl_3$ nanosheets; a) TEM bright field with α-$RuCl_3$ nanosheets on lacey-carbon-Cu grid (the red arrow indicates the direction of the EDX linescan), b) TEM elemental mapping of Ru-K und Cl-K, c) EDX linescan along the longitudinal sheet axis described in a) with plotted counts of Ru-K (green) und Cl-K (red), the rapid increase of counts and the end of the measurement is attributed to a folding of the nanosheet and consequent increase of thickness, d) representative EDX spectrum of α-$RuCl_3$ nanosheet